INTERNATIONAL JOURNAL OF SYSTEMS SCIENCE
https://doi.org/10.1080/00207721.2026.2747877

Taylor & Francis
by informa

Check for updates

Integrated safe trajectory planning and control for high relative degree nonlinear systems: a first-order cbf approach

Chengqian Zhou[a], Jun Yang[b], Yangrui Zhang[b], Yang Yi[a] and Yiding Ji[b]

[a]The College of Information and Artificial Intelligence (College of Industrial Software), Yangzhou University, Yangzhou, People's Republic of China; [b]The Robotics and Autonomous Systems Thrust, Systems Hub, The Hong Kong University of Science and Technology (Guangzhou), Guangzhou, People's Republic of China

ABSTRACT

This paper develops an integrated framework for safe trajectory planning and control of disturbed high relative degree nonlinear systems. The approach combines a composite disturbance-rejection controller with a safety-aware trajectory generator, which performs online re-planning using a safety filter. A disturbance observer estimates unknown external disturbances, and the resulting estimates are incorporated into the tracking control layer to enhance robustness against external disturbances. Implemented as a first-order dynamical system in the feedback loop, the trajectory generator enables enforcement of safety constraints through standard first-order control barrier functions (CBFs), avoiding the complexity and conservativeness of high-order CBF (HoCBF) designs. A CBF-based performance regulation mechanism adjusts the generator's output in response to tracking errors, coordinating safety and performance objectives. The resulting strategy ensures satisfaction of safety specifications for disturbed nonlinear systems with high relative degree while reducing conservativeness and enhancing disturbance rejection. Moreover, the framework can be readily extended to satisfy signal temporal logic (STL) specifications with minor modifications. Numerical simulations demonstrate the effectiveness of the proposed method.

ARTICLE HISTORY
Received 20 May 2026
Accepted 4 October 2026

KEYWORDS
Safety-critical control; signal temporal logic; control barrier function; disturbance rejection; disturbance observer; high relative degree nonlinear systems

1. Introduction

Barrier functions (BFs) are Lyapunov-like functions originally introduced in the context of optimisation and later adopted in control theory for safety verification and forward-invariance analysis of constrained sets (Prajna et al., 2007; Tee et al., 2009). Building on this concept, CBFs have emerged as an effective tool for synthesising safety-critical controllers (Ames et al., 2017). In recent years, CBF-based safety control has received significant attention in both theoretical and application-oriented control research, owing to its effectiveness in a broad range of safety-critical systems (Ames et al., 2017; Bhatia et al., 2025; S. Liu et al., 2025; Z. Liu et al., 2026; Ma et al., 2026; Nguyen & Sreenath, 2016; Tan et al., 2022; Tezuka & Nakamura, 2022; J. Wang et al., 2025; Xiao & Belta, 2022; Xiong et al., 2026). Existing CBF-based methods have been widely developed for state-constraint enforcement, forward-invariance guarantee, and real-time control implementation through quadratic programming (QP). More recently, considerable attention has been devoted to control synthesis under signal temporal logic specifications. Optimisation and MPC-based methods encode temporal and logical requirements into online optimisation problems and can handle relatively general STL specifications (T. Yang et al., 2024; Yu, Gao, et al., 2024). Prescribed-performance and event-triggered approaches have also been developed to achieve STL-constrained control while explicitly addressing transient performance and communication efficiency (Long & Gao, 2024). In parallel, CBF-based methods encode STL predicates and temporal requirements into time-varying barrier functions, providing computationally efficient feedback synthesis with formal satisfaction guarantees (Lindemann & Dimarogonas, 2019a, 2020; Yu, Tan, et al., 2024; W. T. Zhang et al., 2026; Y. Zhang et al., 2026; Zhu & Long, 2025).

Despite the significant progress made in recent years, several challenges still limit the application

CONTACT Jun Yang jy@hkust-gz.edu.cn The Robotics and Autonomous Systems Thrust, Systems Hub, The Hong Kong University of Science and Technology (Guangzhou), Guangzhou 511453, People's Republic of China

© 2026 Informa UK Limited, trading as Taylor & Francis Group

of CBF-based methods to safety-critical control and temporal logic-constrained tasks. Most standard CBF formulations require the safety constraint or logical predicate to have relative degree one with respect to the control input. To handle higher relative degree constraints, high-order control barrier functions (HoCBFs) have been developed (Nguyen & Sreenath, 2016; Tan et al., 2022; Xiao & Belta, 2022). However, HoCBF-based designs generally require the recursive construction of multiple barrier conditions involving higher-order derivatives of the constraint function, which may increase design complexity and conservativeness. Another important challenge arises in the presence of unknown external disturbances and uncertainties, which has motivated the development of various robust CBF-based approaches (Das et al., 2026; Xu, 2018). More specifically, recent studies have combined disturbance observers or disturbance-rejection techniques with CBFs to enhance robustness against disturbances (Alan et al., 2023; Sun et al., 2024; X. Wang et al., 2025; J. Yang et al., 2026; Zhou et al., 2025). By exploiting online disturbance estimates and estimation error information, these approaches can reduce the conservativeness associated with purely worst-case robust designs and improve nominal control performance. More recent developments have further incorporated disturbance estimates into adaptive safety bounds or combined disturbance observation with constructive safe-control designs (Z.-Q. Chen et al., 2026; Z. Yang & Xie, 2025). Nevertheless, direct CBF-based safety enforcement becomes considerably more involved when the safety constraint has high relative degree. In particular, when the relative degree of the safety specification with respect to the disturbance is lower than that with respect to the control input, the disturbance and its higher-order derivatives may enter the high-order barrier conditions (X. Wang et al., 2025; J. Yang et al., 2026), thereby increasing the complexity of robustness analysis and controller implementation.

To address the above challenges, this paper develops an integrated framework for safe trajectory planning and control of disturbed nonlinear systems with high relative degree constraints. The framework consists of two tightly coupled modules: a composite disturbance-rejection controller and a safety-aware trajectory generator. The composite disturbance rejection controller drives the system output toward a desired reference without directly imposing safety constraints. To improve robustness against unknown external disturbances, a disturbance observer is introduced, and the resulting disturbance estimates are incorporated into the control law. The trajectory generator is implemented as a first-order dynamical system embedded in the feedback loop. Its output serves as the reference for the tracking controller and is generated through a CBF-constrained optimisation process to ensure safety satisfaction. This construction allows standard first-order CBFs to be used, thereby avoiding the complexity associated with HoCBF design. To further account for performance requirements, a CBF-based regulation mechanism is integrated into the trajectory generator, allowing adaptive adjustment of its output in response to tracking errors, thus maintaining both performance and constraint satisfaction. In addition, the proposed framework can be extended to handle signal temporal logic specifications through appropriate modifications to the trajectory generation layer. Compared with our previous work (Zhou et al., 2025), where STL constraints were directly encoded by CBFs and the applicability was limited to relative-degree-one systems, the present framework addresses disturbed nonlinear systems with high relative degree constraints in a unified manner. Different from existing approaches that directly impose CBF constraints on the original high relative degree system, the proposed framework relocates safety enforcement to a first-order trajectory-generation layer. This structural reformulation avoids the recursive high-order barrier construction and prevents higher-order disturbance derivatives from entering the safety design. Meanwhile, the tracking and safety layers are coupled through a performance CBF, which explicitly accounts for disturbance-estimation errors and guarantees a prescribed tracking tolerance between the actual output and the generated safe reference. The main contributions of this work are summarised as follows.

(1) An integrated safe trajectory planning and control framework is proposed for disturbed nonlinear systems with high relative degree safety constraints. Different from conventional HoCBF-based methods that directly enforce safety on the original plant dynamics, the proposed method introduces a first-order trajectory generator as the safety interface. Therefore, standard first-order

CBFs can be employed without recursive high-order barrier construction, which reduces design complexity and conservativeness.

(2) A disturbance observer-based tracking layer is combined with a CBF-based performance regulation mechanism. The disturbance estimate is used for compensation in the tracking controller, while the residual estimation error is explicitly incorporated into the performance CBF condition. Consequently, robust safety can be established without introducing higher-order disturbance derivatives into the barrier construction, which considerably simplifies the robustness analysis compared with disturbance-aware HoCBF approaches.

(3) Owing to the modular separation between the tracking layer and the trajectory generation layer, the framework can be extended from state safety constraints to STL specifications by modifying only the trajectory generation layer. This provides a unified implementation architecture for safety-critical and temporal logic constrained tasks under disturbances.

Notation: Throughout this paper, scalars are denoted by non-bold letters, while column vectors are represented by bold letters. The symbol $\mathbb{R}$ denotes the set of real numbers, $\mathbb{R}^n$ represents the n-dimensional real vector space, and $\mathbb{R}_{\geq 0}$ is the set of non-negative real numbers. A continuous function $\alpha_e : (-b, a) \to (-\infty, \infty)$ is said to be an extended class $\mathcal{K}$ function for some $a,\ b > 0$ if it is strictly increasing and $\alpha_e(0) = 0$.

2. Preliminaries and problem formulation

2.1. Control barrier function

Consider the following control affine system

$$\dot{\boldsymbol{x}} = \boldsymbol{f}(\boldsymbol{x}) + \boldsymbol{g}(\boldsymbol{x})\boldsymbol{u} \tag{1}$$

where $\boldsymbol{x} \in \mathbb{R}^n, \boldsymbol{u} \in \mathcal{U} \subseteq \mathbb{R}^m$ denote the state and input, respectively. The functions $\boldsymbol{f}(\boldsymbol{x}) : \mathbb{R}^n \to \mathbb{R}^n$ and $\boldsymbol{g}(\boldsymbol{x}) : \mathbb{R}^n \to \mathbb{R}^{n\times m}$ are locally Lipschitz.

Let the safe set be defined as

$$\mathcal{C} = \{\boldsymbol{x} \in \mathbb{R}^n | b(\boldsymbol{x}) \geq 0\} \tag{2}$$

where $b(\boldsymbol{x}) : \mathbb{R}^n \to \mathbb{R}$ is a continuously differentiable function. The set $\mathcal{C}$ is said to be *forward invariant* with respect to (1) if for each $x(0) \in \mathcal{C}$, the solution $\boldsymbol{x}(t)$ remains within $\mathcal{C}$, for all $t > 0$.

Definition 2.1 (CBF Lindemann & Dimarogonas, 2019a): Given the set $\mathcal{C}$ defined in (2), a differentiable function $b(\boldsymbol{x}, t)$ is referred to as a CBF for (1) if there exists an extended class $\mathcal{K}$ function $\alpha(\cdot)$ such that

$$\sup_{\boldsymbol{u}\in\mathcal{U}} \left[\frac{\partial b^{\mathrm{T}}(\boldsymbol{x})}{\partial \boldsymbol{x}} (\boldsymbol{f}(\boldsymbol{x}) + \boldsymbol{g}(\boldsymbol{x})\boldsymbol{u}) + \alpha(b(\boldsymbol{x})) \right] \geq 0$$

If $b(\boldsymbol{x})$ is a CBF, any Lipschitz continuous controller $\boldsymbol{u}$ satisfying

$$\boldsymbol{u} \in \left\{ \boldsymbol{u} \in \mathcal{U} | \frac{\partial b^{\mathrm{T}}(\boldsymbol{x})}{\partial \boldsymbol{x}} (\boldsymbol{f} + \boldsymbol{g}\boldsymbol{u}) + \alpha(b) \geq 0 \right\} \tag{3}$$

ensures that the set $\mathcal{C}$ is forward invariant.

2.2. Motivation and problem formulation

To illustrate the limitations of conventional CBF-based techniques and motivate the proposed approach, we begin with a representative example. Specifically, consider the mobile robot model (Y. Chen et al., 2019; G. Wang et al., 2024) subject to external disturbances:

$$\begin{cases} \dot{p}_x = v\cos(\theta) + d_x, \\ \dot{p}_y = v\sin(\theta) + d_y, \\ \dot{\theta} = u_\theta \end{cases} \tag{4}$$

where $\boldsymbol{p} = [p_x, p_y]^{\mathrm{T}} \in \mathbb{R}^2$ denotes the robot position in a preset coordinate frame, $v \in \mathbb{R}$ is the linear velocity input, $\theta \in \mathbb{R}$ is the heading angle, and $u_\theta \in \mathbb{R}$ is the angular velocity input. The terms $d_x \in \mathbb{R}$ and $d_y \in \mathbb{R}$ represent external unknown disturbances. Suppose that the robot is required to avoid a circular obstacle centred at $(p_{x,o}, p_{y,o})$ with radius R_o. A natural candidate CBF for this safety requirement is

$$b(\boldsymbol{p}) = (p_x - p_{x,o})^2 + (p_y - p_{y,o})^2 - R_o^2$$

The safety requirement is satisfied if the set

$$\mathcal{C} = \{\boldsymbol{p} \in \mathbb{R}^2 | b(\boldsymbol{p}) \geq 0\}$$

is forward invariant. However, $b(\boldsymbol{p})$ has relative degree two with respect to the control input u_θ in (4). Specifically, the first Lie derivative of $b(\boldsymbol{p})$ along the system dynamics does not explicitly depend on u_θ. Therefore, the standard relative degree-one CBF condition cannot be applied directly, and the constraint-based controller in (3) cannot be constructed to guarantee safety.

A commonly adopted remedy is to employ HoCBFs, which can accommodate higher relative degree constraints. Although effective, HoCBF-based methods still face several limitations. First, the recursive derivation of higher-order derivatives introduces significant computational complexity and design conservatism. Second, higher-order derivatives of external unknown disturbances may also enter the resulting optimisation problem (X. Wang et al., 2025), which further complicates the robustness analysis and disturbance handling. These issues motivate the development of a new robust safety control framework that avoids the use of high-order derivatives, reduces conservativeness, and mitigates the effect of unknown disturbances.

To address the above challenges, we consider the safe control problem for disturbed nonlinear systems. Specifically, the following control-affine model is studied:

$$\begin{cases} \dot{\boldsymbol{x}} = \boldsymbol{f}(\boldsymbol{x}) + \boldsymbol{g}(\boldsymbol{x})\boldsymbol{u} + \boldsymbol{d}(t), \\ \boldsymbol{y} = \boldsymbol{h}(\boldsymbol{x}) \end{cases} \tag{5}$$

where $\boldsymbol{y} \in \mathbb{R}^p$ is the output vector, $\boldsymbol{d}(t) = [d_1(t), \ldots, d_n(t)]^{\mathrm{T}} \in \mathbb{R}^n$ represents an external disturbance. The external disturbance $\boldsymbol{d}(t)$ is assumed to satisfy the following general conditions.

Assumption 2.1: The disturbance $\boldsymbol{d}(t)$ and its derivative $\dot{\boldsymbol{d}}(t)$ are bounded, i.e. $\|\boldsymbol{d}(t)\| \leq \bar{d}$ and $\|\dot{\boldsymbol{d}}(t)\| \leq \bar{d}^*$, where $\bar{d}$ and $\bar{d}^*$ are known positive constants.

3. Integrated safe trajectory planning and control framework

In this section, the proposed integrated safe trajectory planning and control framework is presented for disturbed nonlinear systems with high relative degree safety constraints. The framework consists of two layers: a disturbance-observer-based composite controller and a safety-aware trajectory generator. The overall architecture is illustrated in Figure 1.

3.1. Disturbance observer design and pre-stabilising feedback without safety specifications

To estimate the unknown disturbance $\boldsymbol{d}(t)$ in system (5), we adopt the nonlinear disturbance observer

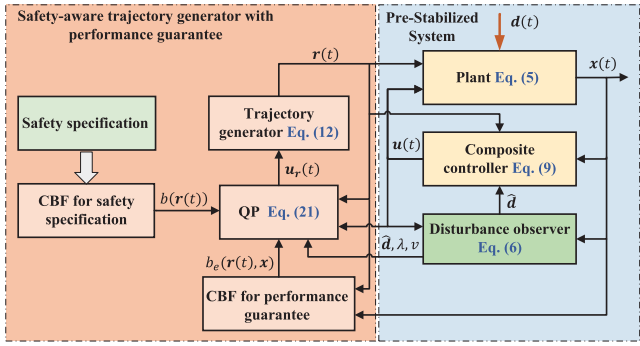


Figure 1. Implementation block diagram of the proposed method.

(W.-H. Chen et al., 2000):

$$\begin{cases} \hat{\boldsymbol{d}} = \lambda(\boldsymbol{x} - \boldsymbol{z}), \\ \dot{\boldsymbol{z}} = \boldsymbol{f}(\boldsymbol{x}) + \boldsymbol{g}(\boldsymbol{x})\boldsymbol{u} + \hat{\boldsymbol{d}} \end{cases} \tag{6}$$

where $\boldsymbol{z}$ is the auxiliary observer state, $\hat{\boldsymbol{d}}$ denotes the estimate of $\boldsymbol{d}$, and λ is a design parameter. Let $\boldsymbol{e}_d = \boldsymbol{d} - \hat{\boldsymbol{d}}$ be the disturbance estimation error, and introduce the Lyapunov candidate $V_{\boldsymbol{e}_d}(t) = \frac{1}{2}\boldsymbol{e}_d^{\mathrm{T}}\boldsymbol{e}_d$. Then,

$$\dot{V}_{\boldsymbol{e}_d}(t) = -\lambda \boldsymbol{e}_d^{\mathrm{T}}\boldsymbol{e}_d + \boldsymbol{e}_d^{\mathrm{T}}\dot{\boldsymbol{d}} \leq -(2\lambda - \nu)V_{\boldsymbol{e}_d}(t) + \frac{(\bar{d}^*)^2}{2\nu} \tag{7}$$

where $\nu > 0$ is a design constant. By choosing $2\lambda - \nu > 0$, one obtains

$$V_{\boldsymbol{e}_d} \leq \mathrm{e}^{-(2\lambda-\nu)t}\left(V_{\boldsymbol{e}_d}(0) - \frac{(\bar{d}^*)^2}{2\nu(2\lambda - \nu)}\right) + \frac{(\bar{d}^*)^2}{2\nu(2\lambda - \nu)} \tag{8}$$

Therefore, $\|\boldsymbol{e}_d\|$ is uniformly ultimately bounded, and its ultimate bound can be reduced by proper selection of ν and λ.

In what follows, we consider stabilising the system output $\boldsymbol{y}$ to an arbitrary fixed point $\boldsymbol{r} \in \mathbb{R}^p$ without imposing safety constraints. Using the disturbance estimate together with a compensation term, the control input is designed in the following composite form:

$$\boldsymbol{u}(t) = \boldsymbol{u}_{\mathrm{nom}}(\boldsymbol{x}, \boldsymbol{r}) + \boldsymbol{u}_d(\boldsymbol{x}, \boldsymbol{r}, \hat{\boldsymbol{d}}) \tag{9}$$

where $\boldsymbol{u}_{\mathrm{nom}}(\boldsymbol{x}, \boldsymbol{r})$ denotes the nominal controller, and $\boldsymbol{u}_d(\boldsymbol{x}, \boldsymbol{r}, \hat{\boldsymbol{d}})$ is the disturbance compensation term. Under the resulting closed-loop dynamics, the disturbed nonlinear system (5) can be represented in the

following pre-stabilised form:

$$\begin{cases} \dot{\boldsymbol{x}} = \boldsymbol{F}(\boldsymbol{x}, \boldsymbol{r}) + \boldsymbol{B}_c(\boldsymbol{x}, \boldsymbol{r})\boldsymbol{e}_d, \\ \boldsymbol{y} = \boldsymbol{h}(\boldsymbol{x}) \end{cases} \tag{10}$$

where $\boldsymbol{F}(\boldsymbol{x}, \boldsymbol{r})$ denotes the nominal pre-stabilised closed-loop vector field, and $\boldsymbol{B}_c(\boldsymbol{x}, \boldsymbol{r})\boldsymbol{e}_d$ characterises the residual disturbance effect induced by the estimation error. In particular, when $\boldsymbol{e}_d = \boldsymbol{0}$, the closed-loop system reduces to the nominal dynamics

$$\dot{\boldsymbol{x}} = \boldsymbol{F}(\boldsymbol{x}, \boldsymbol{r}) \tag{11}$$

which is assumed to achieve the desired output regulation objective with respect to the reference $\boldsymbol{r}$.

Here, $\boldsymbol{B}_c(\boldsymbol{x}, \boldsymbol{r})$ does not denote the input matrix of the original system. Instead, it represents an equivalent gain matrix in the controlled system that characterises how the disturbance estimation error enters the pre-stabilised dynamics. Throughout this paper, $\boldsymbol{B}_c(\boldsymbol{x}, \boldsymbol{r})$ is assumed to be locally Lipschitz in $(\boldsymbol{x}, \boldsymbol{r})$ and bounded on the domain of interest. Therefore, the influence of the unknown disturbance on the closed-loop system is explicitly captured through the estimation error $\boldsymbol{e}_d$.

As a result, the closed-loop dynamics can be viewed as the nominal pre-stabilised system perturbed by a bounded residual term. Consequently, the output $\boldsymbol{y}$ is driven to a neighbourhood of $\boldsymbol{r}$, and the neighbourhood size depends on the disturbance estimation accuracy.

3.2. Safety-aware trajectory generator with performance guarantee

In the previous subsection, a composite controller was constructed to regulate the system output $\boldsymbol{y}$ to a static point $\boldsymbol{r}$ without considering safety constraints. To enforce safety, we introduce a trajectory generator that adjusts $\boldsymbol{r}$ online according to safety specifications encoded by CBFs. Specifically, the trajectory generator is described by

$$\dot{\boldsymbol{r}}(t) = \boldsymbol{u}_r(t), \boldsymbol{r}(\boldsymbol{0}) = \boldsymbol{y}(\boldsymbol{0}) \tag{12}$$

where $\boldsymbol{r}(t) \in \mathbb{R}^p$ denotes the output of the trajectory generator, and $\boldsymbol{u}_r(t) \in \mathbb{R}^p$ is the control input to be designed.

To ensure that the generated trajectory $\boldsymbol{r}(t)$ satisfies the prescribed safety requirements, we impose a CBF constraint through the following online QP:

$$\begin{aligned} \min_{\boldsymbol{u}_r \in \mathbb{R}^p} \quad & (\boldsymbol{u}_r - \boldsymbol{u}_r^{\text{nom}})^{\mathrm{T}} \boldsymbol{H} (\boldsymbol{u}_r - \boldsymbol{u}_r^{\text{nom}}) \\ \text{s.t.} \quad & \frac{\partial b(\boldsymbol{r}(t))}{\partial \boldsymbol{r}}^{\mathrm{T}} \boldsymbol{u}_r \geq -\alpha(b(\boldsymbol{r}(t))) \end{aligned} \tag{13}$$

where $\boldsymbol{H} \succ 0$ is a weighting matrix, $\alpha(\cdot)$ is an extended class $\mathcal{K}$ function, and $\boldsymbol{u}_r^{\text{nom}}$ is a nominal reference controller that drives $\boldsymbol{r}(t)$ toward the desired target in the absence of safety constraints. The function $b(\boldsymbol{r}(t))$ is a continuously differentiable function serving as a primary CBF that encodes the safety constraint. The control input $\boldsymbol{u}_r$ obtained from (13) guarantees the forward invariance of the set

$$C_p = \{\boldsymbol{r}(t) \in \mathbb{R}^p | b(\boldsymbol{r}(t)) \geq 0\}$$

By combining the pre-stabilised closed-loop system (10), the trajectory generator (12), and the control law obtained from (13), the resulting augmented system with state vector $[\boldsymbol{x}(t), \boldsymbol{r}(t)]^{\mathrm{T}}$ can be written as

$$\begin{cases} \dot{\boldsymbol{x}}(t) = \boldsymbol{F}(\boldsymbol{x}, \boldsymbol{r}) + \boldsymbol{B}_c(\boldsymbol{x}, \boldsymbol{r})\boldsymbol{e}_d, \\ \dot{\boldsymbol{r}}(t) = \boldsymbol{u}_r, \\ \boldsymbol{y}(t) = \boldsymbol{h}(\boldsymbol{x}), \boldsymbol{r}(\boldsymbol{0}) = \boldsymbol{y}(\boldsymbol{0}) \end{cases} \tag{14}$$

From (14), it can be concluded that if the controller in (9) is poorly tuned, excessive tracking error may cause the actual output $\boldsymbol{y}(t)$ to violate the intended safety requirement, even when the generated reference $\boldsymbol{r}(t)$ remains safe, as illustrated inFigure 2(a).

To address this issue, we introduce a CBF-based performance regulation mechanism for regulating the generated trajectory. This mechanism explicitly links the generated reference $\boldsymbol{r}(t)$ and the system output $\boldsymbol{y}(t)$. By adjusting $\boldsymbol{r}(t)$ online according to their relative distance, the proposed scheme ensures that $\boldsymbol{r}(t)$ remains within the safety-admissible set while being tracked by $\boldsymbol{y}(t)$ within a prescribed ε-tolerance band, as illustrated in Figure 2(b).

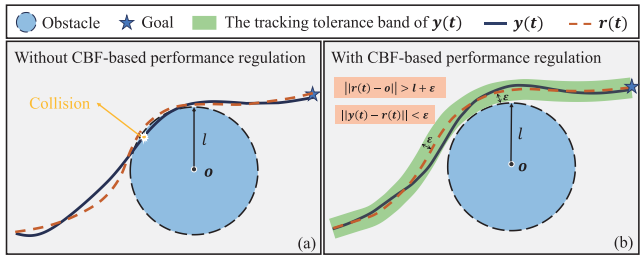


Figure 2. Comparison of the trajectories with and without CBF-based performance regulation mechanism.

To implement the above regulation mechanism, for a given admissible positive error constant ε, a function $b_e(\boldsymbol{r}(t), \boldsymbol{x})$ is constructed as follows:

$$b_e(\boldsymbol{r}(t), \boldsymbol{x}) = \varepsilon - \|\boldsymbol{h}(\boldsymbol{x}) - \boldsymbol{r}(t)\| \tag{15}$$

The set associated with $b_e(\boldsymbol{r}(t), \boldsymbol{x})$ is defined as

$$\mathcal{C}_e = \{\boldsymbol{h}(\boldsymbol{x}), \boldsymbol{r}(t) | b_e(\boldsymbol{r}(t), \boldsymbol{x}) \geq 0\} \tag{16}$$

From the definitions of $b_e(\boldsymbol{r}(t), \boldsymbol{x})$ and the set $\mathcal{C}_e$, it follows that forward invariance of $\mathcal{C}_e$ guarantees

$$\|\boldsymbol{h}(\boldsymbol{x}) - \boldsymbol{r}(t)\| \leq \varepsilon$$

The following theorem establishes a sufficient condition for the forward invariance of $\mathcal{C}_e$.

Theorem 3.1: *Consider the system* (14) *with state vector* $[\boldsymbol{x}, \boldsymbol{r}(t)]^{\mathrm{T}}$. *Suppose that Assumption* 2.1 *holds, and choose positive constants* δ *and* δ_c *such that* $b_e(\boldsymbol{r}(0), \boldsymbol{x}(0)) - \delta V_{e_d}(0) > 0$ *and* $\lambda - \frac{\nu}{2} - \frac{\delta_c}{2} > 0$. *If the input* $\boldsymbol{u}_r$ *satisfies*

$$\begin{aligned}\frac{\partial b_e(\boldsymbol{r}(t), \boldsymbol{x})}{\partial \boldsymbol{r}(t)}^{\mathrm{T}} \boldsymbol{u}_r \geq & -\frac{\partial b_e(\boldsymbol{r}(t), \boldsymbol{x})}{\partial \boldsymbol{x}}^{\mathrm{T}} \boldsymbol{F}(\boldsymbol{x}, \boldsymbol{r}) + \frac{\delta(\bar{d}^*)^2}{2\nu} \\ & + \frac{\|\frac{\partial b_e}{\partial \boldsymbol{x}}^{\mathrm{T}} \boldsymbol{B}_c(\boldsymbol{x}, \boldsymbol{r})\|^2}{4\delta(\lambda - \frac{\nu}{2} - \frac{\delta_c}{2})} - \delta_c b_e(\boldsymbol{r}(t), \boldsymbol{x})\end{aligned} \tag{17}$$

then the set $\mathcal{C}_e$ *is forward invariant.*

Proof: Define an auxiliary function $\bar{b}_e(\boldsymbol{r}(t), \boldsymbol{x}, \boldsymbol{e}_d) = b_e(\boldsymbol{r}(t), \boldsymbol{x}) - \delta V_{e_d}(t)$, where $\delta > 0$ is a constant. According to (7) and (14), we have

$$\begin{aligned}\dot{\bar{b}}_e &= \dot{b}_e - \delta \dot{V}_{e_d} \\ &\geq \frac{\partial b_e}{\partial \boldsymbol{x}}^{\mathrm{T}} (\boldsymbol{F}(\boldsymbol{x}, \boldsymbol{r}) + \boldsymbol{B}_c(\boldsymbol{x}, \boldsymbol{r})\boldsymbol{e}_d) + \frac{\partial b_e}{\partial \boldsymbol{r}}^{\mathrm{T}} \boldsymbol{u}_r \\ &\quad + \delta\left(\lambda - \frac{\nu}{2}\right)\boldsymbol{e}_d^{\mathrm{T}}\boldsymbol{e}_d - \frac{\delta(\bar{d}^*)^2}{2\nu} \\ &= \frac{\partial b_e}{\partial \boldsymbol{x}}^{\mathrm{T}} (\boldsymbol{F}(\boldsymbol{x}, \boldsymbol{r}) + \boldsymbol{B}_c(\boldsymbol{x}, \boldsymbol{r})\boldsymbol{e}_d) + \frac{\partial b_e}{\partial \boldsymbol{r}}^{\mathrm{T}} \boldsymbol{u}_r - \frac{\delta(\bar{d}^*)^2}{2\nu} \\ &\quad + \left(\delta\left(\lambda - \frac{\nu}{2}\right) - \frac{\delta\delta_c}{2}\right)\boldsymbol{e}_d^{\mathrm{T}}\boldsymbol{e}_d + \frac{\delta\delta_c}{2}\boldsymbol{e}_d^{\mathrm{T}}\boldsymbol{e}_d \\ &= \frac{\partial b_e}{\partial \boldsymbol{x}}^{\mathrm{T}} \boldsymbol{F}(\boldsymbol{x}, \boldsymbol{r}) + \frac{\partial b_e}{\partial \boldsymbol{r}}^{\mathrm{T}} \boldsymbol{u}_r - \frac{\delta(\bar{d}^*)^2}{2\nu} \\ &\quad - \frac{\|\frac{\partial b_e}{\partial \boldsymbol{x}}^{\mathrm{T}} \boldsymbol{B}_c(\boldsymbol{x}, \boldsymbol{r})\|^2}{4\delta(\lambda - \frac{\nu}{2} - \frac{\delta_c}{2})} + \frac{\delta\delta_c}{2}\boldsymbol{e}_d^{\mathrm{T}}\boldsymbol{e}_d \\ &\quad + \left\|\sqrt{\delta\left(\lambda - \frac{\nu}{2}\right) - \frac{\delta\delta_c}{2}}\boldsymbol{e}_d^{\mathrm{T}} + \frac{\frac{\partial b_e}{\partial \boldsymbol{x}}^{\mathrm{T}} \boldsymbol{B}_c(\boldsymbol{x}, \boldsymbol{r})}{\sqrt{4\delta(\lambda - \frac{\nu}{2} - \frac{\delta_c}{2})}}\right\|^2 \\ &\geq \frac{\partial b_e}{\partial \boldsymbol{x}}^{\mathrm{T}} \boldsymbol{F}(\boldsymbol{x}, \boldsymbol{r}) + \frac{\partial b_e}{\partial \boldsymbol{r}}^{\mathrm{T}} \boldsymbol{u}_r - \frac{\delta(\bar{d}^*)^2}{2\nu} \\ &\quad - \frac{\|\frac{\partial b_e}{\partial \boldsymbol{x}}^{\mathrm{T}} \boldsymbol{B}_c(\boldsymbol{x}, \boldsymbol{r})\|^2}{4\delta(\lambda - \frac{\nu}{2} - \frac{\delta_c}{2})} + \frac{\delta\delta_c}{2}\boldsymbol{e}_d^{\mathrm{T}}\boldsymbol{e}_d\end{aligned} \tag{18}$$

With the condition (17) in mind, (18) can be written as

$$\dot{\bar{b}}_e \geq -\delta_c b_e + \frac{\delta\delta_c}{2}\boldsymbol{e}_d^{\mathrm{T}}\boldsymbol{e}_d = -\delta_c \bar{b}_e \tag{19}$$

which means that $\bar{b}_e > 0$ when $b_e(\boldsymbol{r}(0), \boldsymbol{x}(0)) - \delta V_{e_d}(0) > 0, \forall t \geq 0$. Hence we have $b_e(\boldsymbol{r}(t), \boldsymbol{x}) > 0$, $\forall t \geq 0$, i.e. the set $\mathcal{C}_e$ is forward invariant. ■

It should be noted that the above safety analysis does not require the disturbance estimation error to have already converged to its ultimate bound. Since the estimation error is explicitly incorporated into the auxiliary barrier function, the forward invariance result remains valid during the observer transient as long as the initial condition in Theorem 3.1 and the CBF condition (17) are satisfied. Moreover, from $\dot{\boldsymbol{e}}_d = \dot{\boldsymbol{d}} - \lambda \boldsymbol{e}_d$, the estimation error dynamics depend on the disturbance variation rather than directly on its magnitude. However, faster disturbance variations increase the required robustness margin and make the CBF condition more restrictive.

Remark 3.1: It is important to note that strict safety of the actual system output $\boldsymbol{y}(t)$ in (5) requires the primary CBF to explicitly account for the maximum allowable tracking error ε induced by the integrated planning and control architecture. In particular, the safe set for the generated reference should be conservatively contracted so that the actual output remains safe even under the worst-case tracking deviation. For example, in a two-dimensional plane, consider a circular obstacle centred at $\boldsymbol{o} \in \mathbb{R}^2$ with radius $l > 0$. A suitable CBF can be defined as

$$b(\boldsymbol{r}(t)) = \|\boldsymbol{r}(t) - \boldsymbol{o}\| - \varepsilon - l \tag{20}$$

This construction enforces a safety margin of ε between $\boldsymbol{r}(t)$ and the obstacle boundary. As illustrated in Figure 2(b), the contracted safe set guarantees that

$\boldsymbol{r}(t)$ maintains a clearance of at least ε from the obstacle. Consequently, if $\|\boldsymbol{y}(t) - \boldsymbol{r}(t)\| \leq \varepsilon$, then the actual output $\boldsymbol{y}(t)$ is guaranteed to remain outside the obstacle region.

Based on the above discussion, consider the disturbed nonlinear system (5), the disturbance observer (6), the composite controller (9), and the trajectory generator (12). Suppose Assumption 2.1 holds, $b(\boldsymbol{r}(0)) > 0$, and select positive constants δ and δ_c such that $b_e(\boldsymbol{r}(0), \boldsymbol{x}(0)) - \delta V_{e_d}(0) > 0$ and $\lambda - \frac{\nu}{2} - \frac{\delta_c}{2} > 0$. If the input $\boldsymbol{u}_r$ of the trajectory generator (12) is generated by solving the following QP:

$$\begin{aligned}
\arg\min_{\boldsymbol{u}_r \in \mathbb{R}^p} \quad & (\boldsymbol{u}_r - \boldsymbol{u}_r^{\text{nom}})^{\mathrm{T}} \boldsymbol{H} (\boldsymbol{u}_r - \boldsymbol{u}_r^{\text{nom}}) \\
\text{s.t.} \quad & \frac{\partial b(\boldsymbol{r}(t))}{\partial \boldsymbol{r}(t)}^{\mathrm{T}} \boldsymbol{u}_r \geq -\alpha(b(\boldsymbol{r}(t))), \qquad (21a) \\
& \frac{\partial b_e(\boldsymbol{r}(t), \boldsymbol{x})}{\partial \boldsymbol{r}}^{\mathrm{T}} \boldsymbol{u}_r \geq -\frac{\partial b_e(\boldsymbol{r}(t), \boldsymbol{x})}{\partial \boldsymbol{x}}^{\mathrm{T}} \boldsymbol{F}(\boldsymbol{x}, \boldsymbol{r}) \\
& \quad + \frac{\delta(\bar{d}^*)^2}{2\nu} \\
& \quad + \frac{\| \frac{\partial b_e}{\partial \boldsymbol{x}}^{\mathrm{T}} \boldsymbol{B}_c(\boldsymbol{x}, \boldsymbol{r}) \|^2}{4\delta(\lambda - \frac{\nu}{2} - \frac{\delta_c}{2})} - \delta_c b_e(\boldsymbol{r}(t), \boldsymbol{x}) \qquad (21b)
\end{aligned}$$

Then, the output $\boldsymbol{y}(t)$ of system (5) is guaranteed to satisfy the prescribed safety constraints.

For practical implementation, the proposed method has a simple online procedure. At each sampling instant, the disturbance observer in (6) is first updated to obtain $\hat{d}$, and the composite control input in (9) is then calculated using the current state and generated reference. Subsequently, the safety and performance CBF conditions are evaluated, and the QP in (21) is solved to obtain u_r, which is used to update the reference according to (12). Therefore, the relatively involved derivations in Theorem 3.1 are mainly required for establishing the safety condition, whereas the online implementation only involves disturbance observation, controller evaluation, and the solution of a first-order CBF-based QP.

4. From safety to signal temporal logic: a path forward

Building upon the integrated safe trajectory planning and control framework developed in the previous section, the proposed method can be further extended to handle more expressive task specifications, particularly those described by STL. This extension is facilitated by the modular design of the framework: the composite disturbance rejection controller (9) provides robust tracking in the presence of disturbances, while the trajectory generator in (12) governs the online generation of reference trajectories subject to the desired temporal logic specifications.

4.1. Signal temporal logic

Before introducing STL, we first recall the notion of a predicate. Given a trajectory $\boldsymbol{x} : \mathbb{R}_{\geq 0} \to \mathbb{R}^n$, a predicate μ is evaluated as either *True* or *False* at time t, and is defined as

$$\mu := \begin{cases} True & \text{if } h_\mu(\boldsymbol{x}(t)) \geq 0, \\ False & \text{if } h_\mu(\boldsymbol{x}(t)) < 0 \end{cases} \qquad (22)$$

where $h_\mu(\boldsymbol{x}) : \mathbb{R}^n \to \mathbb{R}$ is a continuously differentiable predicate function. In this section, we consider the following fragment of STL formulas:

$$\psi := True | \mu | \neg\mu | \psi_1 \wedge \psi_2, \qquad (23a)$$

$$\phi := \phi_1 \wedge \phi_2 | F_{[t_a,t_b]}\psi | G_{[t_a,t_b]}\psi | \psi_1 U_{[t_a,t_b]} \psi_2 \qquad (23b)$$

Here ψ, ψ_1 and ψ_2 are non-temporal formulas, while ϕ, ϕ_1 and ϕ_2 are temporal formulas. The operators $\wedge$ and $\neg$ represent Boolean *Conjunction* and *Negation*, respectively. Moreover $F_{[t_a,t_b]}$, $G_{[t_a,t_b]}$, and $U_{[t_a,t_b]}$ denote the temporal operators *Eventually*, *Always*, and *Until*, respectively, over the interval $[t_a, t_b]$, where $0 \leq t_a < t_b \leq \infty$.

For a continuous-time signal $\boldsymbol{x}(t) : \mathbb{R}_{\geq 0} \to \mathbb{R}^n$, the notation $(\boldsymbol{x}, t) \models \phi$ means that the signal satisfies the STL formula ϕ at time t. The semantics of STL are defined recursively as follows Maler and Nickovic (2004), Donzé and Maler (2010), and Lindemann and Dimarogonas (2019b):

$$\begin{aligned}
& (\boldsymbol{x}, t) \models \mu \Leftrightarrow h_\mu(\boldsymbol{x}(t)) \geq 0, \\
& (\boldsymbol{x}, t) \models \neg\mu \Leftrightarrow \neg((\boldsymbol{x}, t) \models \mu), \\
& (\boldsymbol{x}, t) \models \phi_1 U_{[t_a,t_b]} \phi_2 \Leftrightarrow \exists t' \in [t + t_a, t + t_b], \\
& \qquad (\boldsymbol{x}, t') \models \phi_2 \wedge \forall t'' \in [t, t'], (\boldsymbol{x}, t'') \models \phi_1, \\
& (\boldsymbol{x}, t) \models \phi_1 \wedge \phi_2 \Leftrightarrow ((\boldsymbol{x}, t) \models \phi_1) \wedge ((\boldsymbol{x}, t) \models \phi_2), \\
& (\boldsymbol{x}, t) \models F_{[t_a,t_b]}\phi \Leftrightarrow \exists t' \in [t + t_a, t + t_b], (\boldsymbol{x}, t') \models \phi, \\
& (\boldsymbol{x}, t) \models G_{[t_a,t_b]}\phi \Leftrightarrow \forall t' \in [t + t_a, t + t_b], (\boldsymbol{x}, t') \models \phi
\end{aligned} \qquad (24)$$

Assumption 4.1 (Lindemann & Dimarogonas, 2020): or each predicate μ_l involved in the STL specification, the corresponding predicate function $h_{\mu_l}(\cdot)$, $l \in \{1, \ldots, p\}$, is continuously differentiable and concave on the domain of interest.

Remark 4.1: Assumption 4.1 is introduced to support the STL-to-CBF construction when multiple predicates are combined through smooth lower-bound approximations. Under this assumption, the resulting composite barrier function preserves the concavity property required in the existing STL-CBF constructions based on smooth lower-bound approximations, and the corresponding STL satisfaction argument follows the standard reasoning in STL-CBF-based methods.

4.2. From STL to CBF constraints

The central idea is to encode each STL predicate or temporal constraint into a corresponding primary time-varying CBF $b(\boldsymbol{r}(t), t)$, such that satisfaction of the STL formula is achieved when $\boldsymbol{r}(t)$ remains in the forward-invariant set induced by the CBF. By solving an online QP that enforces the forward invariance of all relevant sets, the trajectory generator ensures STL satisfaction at the reference level. Meanwhile, the robust tracking controller keeps the actual system output $\boldsymbol{y}(t)$ sufficiently close to $\boldsymbol{r}(t)$, so that the STL specifications can be enforced at the output level within a guaranteed tracking error bound.

Following Lindemann and Dimarogonas (2019a, 2020), a time-varying CBF $b(\boldsymbol{r}(t), t)$ can be constructed to represent the mismatch between the desired behaviour specified by the temporal operator and the actual evolution of the reference trajectory in (23b). By combining multiple CBFs, more complex STL specifications can be handled in a unified manner. The construction of $b(\boldsymbol{r}(t), t)$ is briefly reviewed below.

First, for the *Until* operator $\phi = \psi_1 U_{[t_a, t_b]} \psi_2$, we employ the stronger condition $G_{[t_a, t_b]} \psi_1 \wedge F_{[t_b, t_b]} \psi_2$, whose satisfaction guarantees satisfaction of the corresponding Until specification. Based on this construction, the temporal logic formulas in (23b) can be reduced to compositions involving only the *Eventually* and *Always* operators. For the predicates $\mu_i, i = 1, \ldots, p$, let $h_{\mu_i}(\boldsymbol{r})$ denote the corresponding predicate functions. In the following, we outline the design principles for constructing $b(\boldsymbol{r}(t), t)$ for STL specifications in three steps.

Step (I) Consider the STL formulas in (23b) without the *Conjunction* operator. For $\phi_1 = F_{[t_a, t_b]} \mu_1$, the corresponding CBF $b_{\phi_1}(\boldsymbol{r}(t), t)$ should be designed such that

$$b_{\phi_1}(\boldsymbol{r}(t), t_1) \leq h_{\mu_1}(\boldsymbol{r}(t)), \quad \exists t_1 \in [t_a, t_b]$$

Similarly, for $\phi_2 = G_{[t_a, t_b]} \mu_1$, $b_{\phi_2}(\boldsymbol{r}(t), t)$ should satisfy

$$b_{\phi_2}(\boldsymbol{r}(t), t_1) \leq h_{\mu_1}(\boldsymbol{r}(t)), \quad \forall t_1 \in [t_a, t_b]$$

Step (II) Consider the STL formulas in (23b) with *Conjunction* operator. To encode the *Conjunction* operator in (23b), we employ a smooth lower bound approximation. For p functions $b_i(\boldsymbol{r}(t), t), i = 1, \ldots, p$, define

$$b(\boldsymbol{r}(t), t) = -\frac{1}{\kappa} \ln \left(\sum_{i=1}^{p} \mathrm{e}^{-\kappa b_i(\boldsymbol{r}(t), t)} \right) \tag{25}$$

where $\kappa > 0$ is a constant. It is straightforward to derive that $b(\boldsymbol{r}(t), t) \approx \min\{b_1(\boldsymbol{r}(t), t), \ldots, b_p(\boldsymbol{r}(t), t)\}$ and the approximation accuracy improves as κ increases, i.e. $\lim_{\kappa \to \infty} -\frac{1}{\kappa} \ln(\sum_{i=1}^{p} \exp(-\kappa b_i(x, t))) = \min_{i \in \{1, \ldots, p\}} b_i(x, t)$. For any finite κ, the smooth lower bound satisfies $-\frac{1}{\kappa} \ln(\sum_{i=1}^{p} \mathrm{e}^{-\kappa b_i(\boldsymbol{r}(t), t)}) \leq \min\{b_1(\boldsymbol{r}(t), t), \ldots, b_p(\boldsymbol{r}(t), t)\}$, which implies that $b(\boldsymbol{r}(t), t) > 0$ implies that $b_i(\boldsymbol{r}(t), t) > 0, i = 1, \ldots, p$.

Here, $\kappa > 0$ is a smoothing parameter that determines the trade-off between smoothness and approximation accuracy. A larger κ provides a tighter approximation to the minimum function, whereas an excessively large value may lead to numerical sensitivity in evaluating the exponential terms. Thus, κ should be chosen sufficiently large to achieve the desired approximation accuracy while maintaining numerical robustness.

Let $\psi = \mu_1 \wedge \cdots \wedge \mu_p$. For $\phi_1 = F_{[t_a, t_b]} \psi$, we first design corresponding CBFs $b_i(\boldsymbol{r}(t), t), i = 1, \ldots, p$ such that

$$b_i(\boldsymbol{r}(t), t_1) \leq h_{\mu_i}(\boldsymbol{r}(t)), \quad \exists t_1 \in [t_a, t_b]$$

Then, by using the smooth lower bound approximation in (25), the CBF $b_{\phi_1}(\boldsymbol{r}(t), t)$ associated with ϕ_1 is given by

$$b_{\phi_1}(\boldsymbol{r}(t), t) = -\frac{1}{\kappa} \ln(\mathrm{e}^{-\kappa b_{\mu_1}(\boldsymbol{r}(t), t)} + \cdots + \mathrm{e}^{-\kappa b_{\mu_p}(\boldsymbol{r}(t), t)})$$

For $\phi_2 = G_{[t_a,t_b]}\psi$, choose $b_{\mu_i}(\boldsymbol{r}(t),t), i=1,\dots,p$ such that

$$b_{\mu_i}(\boldsymbol{r}(t),t_1) \le h_{\mu_i}(\boldsymbol{r}(t)), \quad \forall t_1 \in [t_a,t_b]$$

Similarly, the corresponding $b(\boldsymbol{r}(t),t)$ is chosen as

$$b_{\phi_2}(\boldsymbol{r}(t),t) = -\frac{1}{\kappa}\ln(\mathrm{e}^{-\kappa b_{\mu_1}(\boldsymbol{r}(t),t)} + \cdots + \mathrm{e}^{-\kappa b_{\mu_p}(\boldsymbol{r}(t),t)})$$

Step (III) Consider the conjunction of multiple temporal logic formulas, i.e. $\phi = \phi_1 \wedge \cdots \wedge \phi_n$. In this case, $b(\boldsymbol{r}(t),t)$ can be chosen as

$$b(\boldsymbol{r}(t),t) = -\frac{1}{\kappa}\ln(\mathrm{e}^{-\kappa b_1(\boldsymbol{r}(t),t)} + \cdots + \mathrm{e}^{-\kappa b_n(\boldsymbol{r}(t),t)}) \tag{26}$$

where $b_i(\boldsymbol{r}(t),t), i=1,\dots,n$ are constructed according to Steps (I) and (II).

Thus, for a given STL formula in (23b), a corresponding CBF can be constructed following Steps (I)–(III).

4.3. QP-based STL satisfaction

Once the time-varying CBF $b(\boldsymbol{r},t)$ has been constructed for the given STL specification, the trajectory generator input $\boldsymbol{u}_r$ can be obtained by a straightforward modification of the QP in (21).

Consider the disturbed nonlinear system (5) subject to an STL specification in (23), together with the disturbance observer (6), the composite controller (9), and the trajectory generator (12). Suppose that Assumption 2.1 holds, $b(\boldsymbol{r}(0),0) > 0$, and let δ and δ_c be positive constants satisfying $b_e(\boldsymbol{r}(0),\boldsymbol{x}(0)) - \delta V_{e_d}(0) > 0, \lambda - \frac{\nu}{2} - \frac{\delta_c}{2} > 0$. If $\boldsymbol{u}_r$ is obtained by solving

$$\begin{aligned}
\arg\min_{\boldsymbol{u}_r\in\mathbb{R}^p} \quad & \boldsymbol{u}_r^{\mathrm{T}}\boldsymbol{H}\boldsymbol{u}_r \\
\text{s.t.} \quad & \frac{\partial b(\boldsymbol{r}(t),t)}{\partial \boldsymbol{r}(t)}^{\mathrm{T}}\boldsymbol{u}_r + \frac{\partial b(\boldsymbol{r}(t),t)}{\partial t} \\
& \quad \ge -\alpha(b(\boldsymbol{r}(t),t)), \qquad (27a) \\
& \frac{\partial b_e(\boldsymbol{r}(t),\boldsymbol{x})}{\partial \boldsymbol{r}}^{\mathrm{T}}\boldsymbol{u}_r \ge -\frac{\partial b_e(\boldsymbol{r}(t),\boldsymbol{x})}{\partial \boldsymbol{x}}^{\mathrm{T}} \\
& \quad \times \boldsymbol{F}(\boldsymbol{x},\boldsymbol{r}) + \frac{\delta(\bar{d}^*)^2}{2\nu} \\
& \quad + \frac{\|\frac{\partial b_e}{\partial \boldsymbol{x}}^{\mathrm{T}}\boldsymbol{B}_c(\boldsymbol{x},\boldsymbol{r})\|^2}{4\delta(\lambda - \frac{\nu}{2} - \frac{\delta_c}{2})} - \delta_c b_e(\boldsymbol{r}(t),\boldsymbol{x}) \\
& \qquad (27b)
\end{aligned}$$

then the trajectory generator output $\boldsymbol{r}(t)$ satisfies the given STL specification, and the system output $\boldsymbol{y}(t)$ tracks $\boldsymbol{r}(t)$ with tracking error satisfying $\|\boldsymbol{y}(t) - \boldsymbol{r}(t)\| \le \varepsilon, \forall t \ge 0$.

Remark 4.2: The proposed integrated safe trajectory planning and control framework guarantees that the system output $\boldsymbol{y}(t)$ tracks the STL compliant reference trajectory $\boldsymbol{r}(t)$ within a prescribed error bound ε. However, since the STL specification is formally enforced only at the reference level, strict satisfaction by $\boldsymbol{y}(t)$ is not guaranteed in general. This issue becomes particularly relevant when the robustness degree (Donzé & Maler, 2010; Lindemann & Dimarogonas, 2019b, 2020) of $\boldsymbol{r}(t)$ with respect to the STL specification is close to zero, in which case even small tracking deviations may lead to violations. A practical and widely adopted approach to mitigate this issue is to introduce a robustness margin when verifying STL specifications for $\boldsymbol{r}(t)$. For example, the predicates in the STL formula can be tightened by requiring $h_\mu(\boldsymbol{r}(t)) \ge \varepsilon$, so that any signal evolving within an ε-neighbourhood of $\boldsymbol{r}(t)$, including $\boldsymbol{y}(t)$, also satisfies the original specification. It is noted that the relation between the required robustness margin and the tracking error is generally not explicit, since it depends on the specific structure of the STL formula, including the temporal operators and logical compositions involved. Nevertheless, such predicate tightening provides a practically effective way to improve the reliability of STL satisfaction under bounded tracking uncertainty.

5. Simulation results

The effectiveness of the proposed integrated safe trajectory planning and control framework is evaluated through numerical simulations on a mobile robot described by the nonlinear model in (4). Following the modelling approach in G. Wang et al. (2024) and X. Wang et al. (2026), the linear velocity v is treated as an internal state with a prescribed initial value, and an auxiliary dynamic equation $\dot{v} = u_v$ is introduced to regulate the dynamics of v. Let $\boldsymbol{p}_1 = [v\cos(\theta), v\sin(\theta)]^{\mathrm{T}}$. Then, system (4) can be rewritten as

$$\begin{cases} \dot{\boldsymbol{p}} = \boldsymbol{p}_1 + \boldsymbol{d}, \\ \dot{\boldsymbol{p}}_1 = \boldsymbol{G}\boldsymbol{u} \end{cases} \tag{28}$$

where $\boldsymbol{p} = [p_x, p_y]^{\mathrm{T}} \in \mathbb{R}^2$, $\boldsymbol{u} = [u_v, u_\theta]^{\mathrm{T}}$, $\boldsymbol{d} = [d_x, d_y]^{\mathrm{T}}$, and $\boldsymbol{G} = [\cos(\theta), -v\sin(\theta); \sin(\theta), v\cos(\theta)]$.

Under the assumption that v remains nonzero during task execution (G. Wang et al., 2024), the control input

$$\boldsymbol{u} = \boldsymbol{G}^{-1}(-k_1(\boldsymbol{p} - \boldsymbol{r}) - k_2(\boldsymbol{p}_1 + \hat{\boldsymbol{d}}))$$

drives the system output $\boldsymbol{p}$ to a neighbourhood of the desired fixed point $\boldsymbol{r}$.

The parameters are selected according to the following general guidelines. The observer gain λ determines the convergence rate of the disturbance estimation error and is selected together with ν and δ_c to satisfy $\lambda - \nu/2 - \delta_c/2 > 0$. The tracking gains k_1 and k_2 determine the nominal second-order tracking dynamics and can be selected according to the desired natural frequency and damping ratio. The parameters δ, ν, and δ_c are further selected to satisfy the conditions in Theorem 3.1, while ε is determined according to the allowable tracking error and the required safety margin. In general, the parameters are tuned to balance disturbance estimation speed, tracking performance, robustness, and control effort. In this simulation, the parameters are set to $\lambda = 6$, $k_1 = 4.6$, and $k_2 = 2.5$. The unknown disturbances are given by $d_x = \sin(0.5t)\mathrm{e}^{-t}$, $d_y = \cos(0.5t)\mathrm{e}^{-t}$.

To provide a representative and technically relevant benchmark, the HoCBF-based method in X. Wang et al. (2025) is selected for comparison. HoCBFs constitute a standard approach for enforcing high relative degree safety constraints, while the method in X. Wang et al. (2025) further addresses safety-critical control of nonlinear systems subject to unmatched disturbances, which is closely related to the problem considered in this paper. More importantly, the proposed method and X. Wang et al. (2025) adopt fundamentally different mechanisms for handling high relative degree safety constraints: the latter directly enforces safety on the system output through high-order barrier conditions, whereas the proposed method transfers the safety enforcement to a first-order trajectory generator. Therefore, this comparison directly evaluates the effect of avoiding high-order barrier constructions in terms of conservativeness and task feasibility.

5.1. Trajectory safety enforcement under disturbances

In the first scenario, the proposed method is evaluated for safety enforcement in the presence of unknown disturbances. The robot is assigned a persistent inspection task in a planar environment. The desired reference trajectory is given by $\boldsymbol{p}^d(t) = [0.5t,\ 25\sin(0.05t)]^{\mathrm{T}}$, which corresponds to a sinusoidal scanning motion. This reference is processed by the trajectory generator (12), which computes a safety-admissible intermediate trajectory $\boldsymbol{r}(t)$ by solving the QP (21). The nominal control input for the generator is set as $\boldsymbol{u}_r^{\mathrm{nom}} = [0.5, 1.25\cos(0.05t)]^{\mathrm{T}} - \boldsymbol{r} - \boldsymbol{p}^d$, and the error constant is selected as $\varepsilon = 0.7$.

Figure 3 compares the path profiles obtained by the proposed method and the HoCBF-based approach. Although both methods maintain safety under disturbances, the HoCBF-based method exhibits more conservative behaviour near the boundary of the danger zone. In contrast, the proposed method allows the system to track the desired path more closely while remaining within the admissible region. Figure 4 shows the evolution of $\|\boldsymbol{p}(t) - \boldsymbol{r}(t)\|$, which remains strictly bounded under the proposed approach due to the CBF-based performance regulation mechanism integrated into the trajectory generator. The disturbance estimation errors are presented in Figure 6. Both estimation error components rapidly converge to a small neighbourhood of zero despite the time-varying disturbances, demonstrating the effectiveness of the disturbance observer. Figure 5 shows the corresponding control responses. The heading angular velocity u_θ exhibits short corrective transients when the robot changes its motion direction or approaches safety-critical regions, while the linear velocity v varies smoothly during the task. Both control signals remain bounded, indicating that the safety modification does not introduce excessive control actions.

5.2. STL-constrained task enforcement under disturbances

In the second scenario, the proposed framework is evaluated on a more complex task described by STL. Specifically, we consider a navigation problem involving sequential goal-reaching requirements together with obstacle avoidance. The STL specification in (29) captures both the timed access requirements and

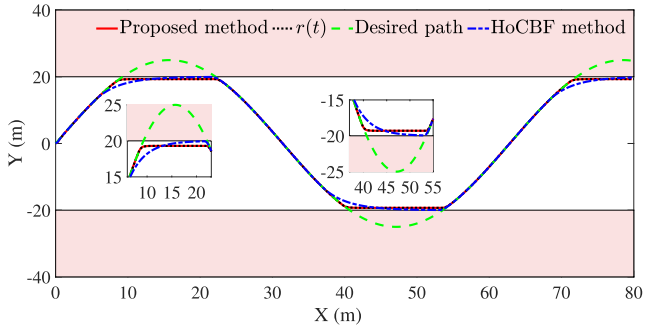


Figure 3. Path profiles under the HoCBF and the proposed method, where the pink area is designated as the danger zone.

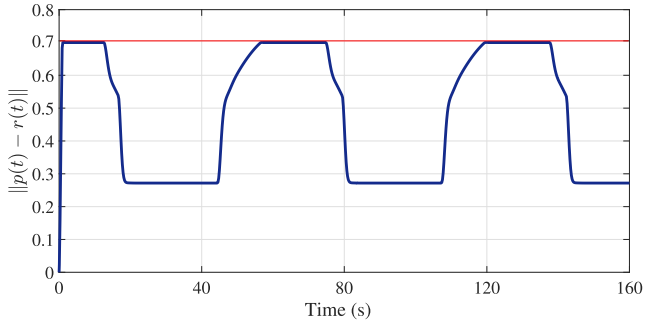


Figure 4. The error curve between the actual position $\boldsymbol{p}(t)$ and the trajectory generator $\boldsymbol{r}(t)$.

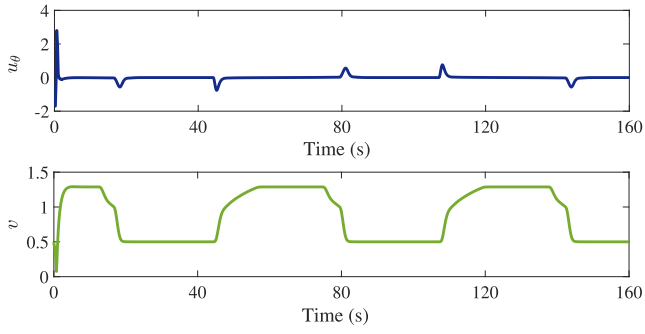


Figure 5. Control responses of the heading angular velocity u_θ and the linear velocity v.

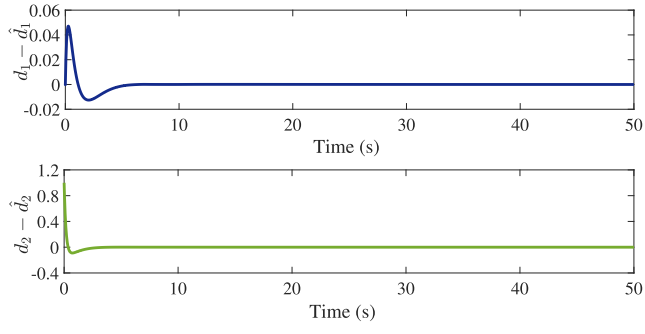


Figure 6. Estimated errors of the unknown disturbances.

the safety requirements. Consider a planar environment containing five obstacle regions and three target regions. The task description is as follows:

Task I: Sequential access tasks with deadlines

The robot is tasked with starting from the origin, reaching goal 1 within 50 seconds, and remaining at goal 1 for 5 seconds. Next, the robot must reach goal 2 within the subsequent 45 seconds and stay there for 5 seconds. Finally, the robot should arrive at goal 3 within the following 40 seconds and remain there indefinitely. The three target areas are defined as follows:

$$\text{goal 1}: \|\boldsymbol{p}-\boldsymbol{p}_{g_1}\| < \varrho_1, \text{goal 2}: \|\boldsymbol{p}-\boldsymbol{p}_{g_2}\| < \varrho_2,$$
$$\text{goal 3}: \|\boldsymbol{p}-\boldsymbol{p}_{g_3}\| < \varrho_3, \text{origin}: \|\boldsymbol{p}-\boldsymbol{p}_o\| < \varrho_o$$

where $\boldsymbol{p}_{g_1} = [10,10]^{\mathrm{T}}$, $\boldsymbol{p}_{g_2} = [22,6]^{\mathrm{T}}$, $\boldsymbol{p}_{g_3} = [15,0]^{\mathrm{T}}$, $\boldsymbol{p}_o = [0,0]^{\mathrm{T}}$, and $\varrho_1 = 1$, $\varrho_2 = 1$, $\varrho_3 = 1$, and $\varrho_o = 0.5$.

Task II: Obstacle avoidance

During task execution, the robot is required to avoid all obstacle regions while navigating toward the target regions. The environment includes five obstacle areas, which are described as follows:

$$\text{obs 1}: \|\boldsymbol{p}-\boldsymbol{p}_{o_1}\| < \varrho_{o_1}, \text{obs 2}: \|\boldsymbol{p}-\boldsymbol{p}_{o_2}\| < \varrho_{o_2},$$
$$\text{obs 3}: \|\boldsymbol{p}-\boldsymbol{p}_{o_3}\| < \varrho_{o_3},$$
$$\text{obs 4}: \|\boldsymbol{p}-\boldsymbol{p}_{o_4}\| < \varrho_{o_4}, \text{obs 5}: \|\boldsymbol{p}-\boldsymbol{p}_{o_5}\| < \varrho_{o_5}$$

where $\boldsymbol{p}_{o_1} = [2,3]^{\mathrm{T}}$, $\boldsymbol{p}_{o_2} = [7,5]^{\mathrm{T}}$, $\boldsymbol{p}_{o_3} = [12,6.5]^{\mathrm{T}}$, $\boldsymbol{p}_{o_4} = [15,8]^{\mathrm{T}}$, $\boldsymbol{p}_{o_5} = [17,4.5]^{\mathrm{T}}$, and $\varrho_{o_1} = 2$, $\varrho_{o_2} = 3$, $\varrho_{o_3} = 1$, $\varrho_{o_4} = 1.5$, $\varrho_{o_5} = 2.5$.

The corresponding STL formula describing Tasks I and II can be expressed as

$$\Theta = \phi_1 \wedge \phi_2 \wedge \phi_3 \wedge \phi_{obs1} \wedge \phi_{obs2} \wedge \phi_{obs3} \wedge \phi_{obs4} \wedge \phi_{obs5} \tag{29}$$

where $\phi_1 = G_{[50,55]}(\text{goal1})$, $\phi_2 = G_{[100,105]}(\text{goal2})$, and $\phi_3 = G_{[145,170]}(\text{goal3})$ encode the goal-reaching requirements in Task I, whereas $\phi_{obs1} = G_{[0,170]}(\neg\text{obs1})$, $\phi_{obs2} = G_{[0,170]}(\neg\text{obs2})$, $\phi_{obs3} = G_{[0,170]}(\neg\text{obs3})$, $\phi_{obs4} = G_{[0,170]}(\neg\text{obs4})$, and $\phi_{obs5} = G_{[0,170]}(\neg\text{obs5})$ encode the obstacle-avoidance requirements in Task II. Specifically, we require the tracking error in the tracking layer to remain within 0.5, i.e. $\|\boldsymbol{p}(t)-\boldsymbol{r}(t)\| \le 0.5$.

The resulting trajectories under the two control strategies are shown in Figures 7 and 8, respectively. As

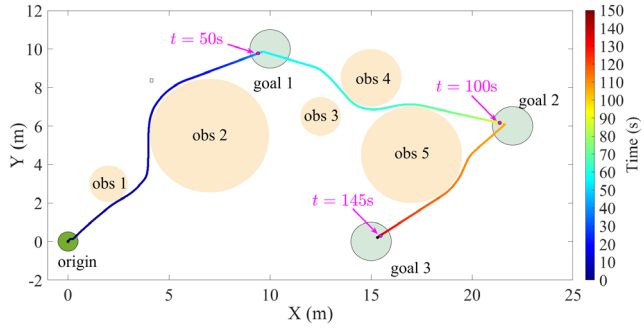


Figure 7. System trajectory under STL specification (29) using the proposed method.

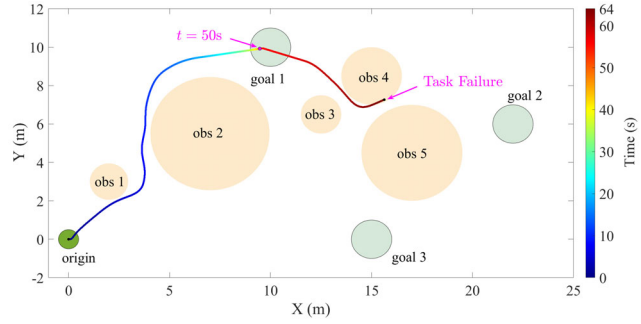


Figure 8. System trajectory under STL specification (29) using the HoCBF method.

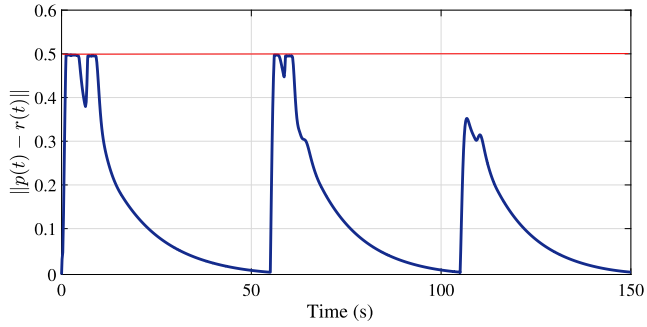


Figure 9. The error curve between actual position $\boldsymbol{p}(t)$ and trajectory generator $\boldsymbol{r}(t)$.

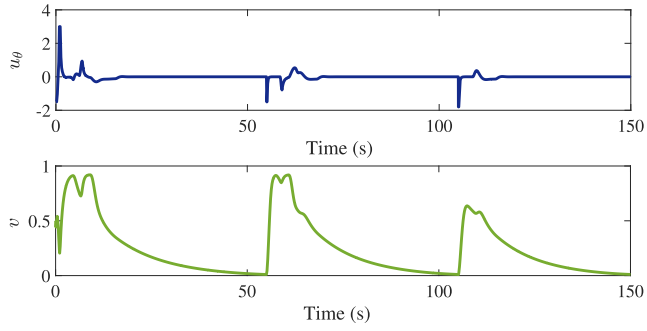


Figure 10. The heading angle velocity u_θ and the linear velocity input v.

shown in Figure 7, the proposed method enables the robot to follow the trajectory generator output, satisfy the STL specification, and maintain safety throughout the task. In contrast, Figure 8 shows that the HoCBF-based method successfully reaches the first target but subsequently fails when passing through the narrow region formed by multiple obstacles. The high-order barrier constraints become more restrictive in this region, substantially reducing the admissible motion directions and preventing continued execution of the temporal task. Figure 9 presents the tracking error between the actual position and the generated trajectory. Although transient increases occur when the trajectory generator changes its motion toward a new target or modifies the reference for obstacle avoidance, the error remains below the prescribed bound of 0.5 throughout the task. This confirms that the performance CBF coordinates the trajectory generation and tracking layers even during relatively rapid reference adjustments. The corresponding control responses are shown in Figure 10. The heading angular velocity mainly exhibits transient corrective actions during changes in motion direction, whereas the linear velocity increases during inter-target motion and decreases as the robot approaches the required target regions. Both signals remain bounded throughout the task. These results show that the proposed method achieves the STL-constrained motion without inducing persistent high-frequency or excessively large control actions.

6. Conclusion

This paper presented an integrated framework for safe trajectory planning and control of disturbed nonlinear systems with high relative degree. By combining a disturbance-rejection controller with a safety-aware first-order trajectory generator, the proposed method enables safety enforcement using standard first-order CBFs, thereby avoiding the high-order barrier construction and disturbance derivatives required by conventional HoCBF-based approaches. Disturbance estimation is incorporated into the tracking layer, while the trajectory generator explicitly accounts for estimation errors to coordinate safety and tracking performance under disturbances. Moreover, the modular framework can be extended to STL specifications by modifying the trajectory-generation layer. Simulation

results demonstrated the effectiveness and reduced conservativeness of the proposed method. Future work will extend the framework to nonlinear systems with input constraints, model uncertainties, and more general disturbance structures, together with the corresponding feasibility and robustness analysis.

Author contributions

CRediT: **Chengqian Zhou:** Conceptualization, Formal analysis, Methodology, Validation, Writing – original draft, Writing – review & editing; **Jun Yang:** Conceptualization, Methodology, Supervision, Writing – review & editing; **Yangrui Zhang:** Conceptualization, Writing – review & editing; **Yang Yi:** Conceptualization, Writing – review & editing; **Yiding Ji:** Writing – review & editing

Disclosure statement

No potential conflict of interest was reported by the author(s).

Data availability statement

Data sharing is not applicable to this article as no data sets were generated or analysed during the current study.

References

Alan, A., Molnar, T. G., Daş, E., Ames, A. D., & Orosz, G. (2023). Disturbance observers for robust safety-critical control with control barrier functions. *IEEE Control Systems Letters*, *7*, 1123–1128. https://doi.org/10.1109/LCSYS.2022.3232059

Ames, A. D., Xu, X., Grizzle, J. W., & Tabuada, P. (2017). Control barrier function based quadratic programs for safety critical systems. *IEEE Transactions on Automatic Control*, *62*(8), 3861–3876. https://doi.org/10.1109/TAC.2016.2638961

Bhatia, P., Roy, S. B., Sujit, P. B., Alvarez, L. M., & Mcfadyen, A. (2025). Decentralized collision avoidance and global connectivity maintenance using nested control barrier functions. *International Journal of Systems Science*, *57*(11), 3532–3547. https://doi.org/10.1080/00207721.2025.2583240

Chen, W.-H., Ballance, D. J., Gawthrop, P. J., & O'Reilly, J. (2000). A nonlinear disturbance observer for robotic manipulators. *IEEE Transactions on Industrial Electronics (1982)*, *47*(4), 932–938. https://doi.org/10.1109/41.857974

Chen, Y., Li, Z., Kong, H., & Ke, F. (2019). Model predictive tracking control of nonholonomic mobile robots with coupled input constraints and unknown dynamics. *IEEE Transactions on Industrial Informatics*, *15*(6), 3196–3205. https://doi.org/10.1109/TII.9424

Chen, Z.-Q., Tao, J., Lin, M., Su, C.-Y., Lu, R., & Liu, Y.-H. (2026). Constructive design of disturbance observer-based safe control for strict-feedback nonlinear systems with disturbances. *ISA Transactions*, *168*, 704–711. https://doi.org/10.1016/j.isatra.2025.11.041

Das, E., Nanayakkara, R., Tan, X., Bena, R. M., Burdick, J. W., Tabuada, P., & A. D. Ames (2026). Safe navigation under state uncertainty: Online adaptation for robust control barrier functions. *IEEE Robotics and Automation Letters*, *11*(3), 3398–3405. https://doi.org/10.1109/LRA.2026.3653366

Donzé, A., & Maler, O. (2010). Robust satisfaction of temporal logic over real-valued signals. In *International conference on formal modeling and analysis of timed systems* (pp. 92–106). Springer Berlin Heidelberg.

Lindemann, L., & Dimarogonas, D. V. (2019a). Control barrier functions for signal temporal logic tasks. *IEEE Control Systems Letters*, *3*(1), 96–101. https://doi.org/10.1109/LCSYS.7782633

Lindemann, L., & Dimarogonas, D. V. (2019b). Feedback control strategies for multi-agent systems under a fragment of signal temporal logic tasks. *Automatica*, *106*, 284–293. https://doi.org/10.1016/j.automatica.2019.05.013

Lindemann, L., & Dimarogonas, D. V. (2020). Barrier function based collaborative control of multiple robots under signal temporal logic tasks. *IEEE Transactions on Control of Network Systems*, *7*(4), 1916–1928. https://doi.org/10.1109/TCNS.6509490

Liu, S., Yu, Z., & Gao, D. (2025). Safe reinforcement learning for cooperative tracking consensus problem of discrete-time multiagent systems with control barrier functions. *International Journal of Systems Science*, *56*(12), 2889–2909. https://doi.org/10.1080/00207721.2025.2461016

Liu, Z., Liu, Y., & Wang, Y. (2026). Finite-time output safe control of uncertain nonlinear systems. *International Journal of Systems Science*, *57*(2), 547–560. https://doi.org/10.1080/00207721.2025.2504650

Long, L., & Gao, G. (2024). Dynamic event-triggered prescribed performance control for nonlinear systems with signal temporal logic. *International Journal of Robust and Nonlinear Control*, *34*(7), 4753–4768. https://doi.org/10.1002/rnc.v34.7

Ma, Q., Li, J., Liu, Q., Qin, J., & Sun, J. (2026). Enhanced safe control for arbitrary relative degree: A generalized discrete-time CBF approach. *Automatica*, *189*, Article 113026. https://doi.org/10.1016/j.automatica.2026.113026

Maler, O., & Nickovic, D. (2004). Monitoring temporal properties of continuous signals. In *International symposium on formal techniques in real-time and fault-tolerant systems* (pp. 152–166). Springer Berlin Heidelberg.

Nguyen, Q., & Sreenath, K. (2016). Exponential control barrier functions for enforcing high relative-degree safety-critical constraints. In *2016 American control conference (ACC)* (pp. 322–328). IEEE.

Prajna, S., Jadbabaie, A., & Pappas, G. J. (2007). A framework for worst-case and stochastic safety verification using barrier certificates. *IEEE Transactions on Automatic Control*, *52*(8), 1415–1428. https://doi.org/10.1109/TAC.2007.902736

Sun, J., Yang, J., & Zeng, Z. (2024). Safety-critical control with control barrier function based on disturbance observer. *IEEE Transactions on Automatic Control*, *69*(7), 4750–4756. https://doi.org/10.1109/TAC.2024.3352707

Tan, X., Cortez, W. S., & Dimarogonas, D. V. (2022). High-order barrier functions: Robustness, safety, and performance-critical control. *IEEE Transactions on Automatic Control*, *67*(6), 3021–3028. https://doi.org/10.1109/TAC.2021.3089639

Tee, K. P., Ge, S. S., & Tay, E. H. (2009). Barrier Lyapunov functions for the control of output-constrained nonlinear systems. *Automatica*, *45*(4), 918–927. https://doi.org/10.1016/j.automatica.2008.11.017

Tezuka, I., & Nakamura, H. (2022). Strict zeroing control barrier function for continuous safety assist control. *IEEE Control Systems Letters*, *6*, 2108–2113. https://doi.org/10.1109/LCSYS.2021.3138526

Wang, G., Wang, X., & Li, S. (2024). A guidance module based formation control scheme for multi-mobile robot systems with collision avoidance. *IEEE Transactions on Automation Science and Engineering*, *21*(1), 382–393. https://doi.org/10.1109/TASE.2022.3228397

Wang, J., Tian, Z., Sun, J., Yang, J., & Li, S. (2025). Event-triggered safety-critical model predictive control for underactuated overhead cranes. *IEEE Transactions on Industrial Informatics*, *21*(9), 6857–6867. https://doi.org/10.1109/TII.2025.3567405

Wang, X., Wang, J., Chen, Y.-Y., Ma, Y., & Li, S. (2026). Hierarchical consensus of constrained second-order multi-agent systems with application to formation of multiple mobile robots. *IEEE Transactions on Automatic Control*, *71*(2), 886–901. https://doi.org/10.1109/TAC.2025.3602134

Wang, X., Yang, J., Liu, C., Yan, Y., & Li, S. (2025). Safety-critical disturbance rejection control of nonlinear systems with unmatched disturbances. *IEEE Transactions on Automatic Control*, *70*(4), 2722–2729. https://doi.org/10.1109/TAC.2024.3496572

Xiao, W., & Belta, C. (2022). High-order control barrier functions. *IEEE Transactions on Automatic Control*, *67*(7), 3655–3662. https://doi.org/10.1109/TAC.2021.3105491

Xiong, Y., Zhai, D., & Xia, Y. (2026). Robust safety-critical control design for robotic systems under input disturbances with multiple time-varying constraints. *International Journal of Systems Science*. https://doi.org/10.1080/00207721.2026.2623179

Xu, X. (2018). Constrained control of input–output linearizable systems using control sharing barrier functions. *Automatica*, *87*, 195–201. https://doi.org/10.1016/j.automatica.2017.10.005

Yang, J., Wang, X., Yu, X., Li, S., & Guo, L. (2026). An overview on safety-critical control under disturbances: A control barrier function approach. *IEEE/ASME Transactions on Mechatronics*. https://doi.org/10.1109/TMECH.2026.3666590

Yang, T., Zou, Y., Li, S., Yin, X., & Jia, T. (2024). Signal temporal logic synthesis under model predictive control: A low complexity approach. *Control Engineering Practice*, *143*, Article 105782. https://doi.org/10.1016/j.conengprac.2023.105782

Yang, Z., & Xie, L. (2025). Disturbance observer-parameterized control barrier function with adaptive safety bounds. *IEEE Control Systems Letters*, *8*, 3380–3385. https://doi.org/10.1109/LCSYS.2025.3535379

Yu, P., Gao, Y., Jiang, F. J., Johansson, K. H., & Dimarogonas, D. V. (2024). Online control synthesis for uncertain systems under signal temporal logic specifications. *The International Journal of Robotics Research*, *43*(6), 765–790. https://doi.org/10.1177/02783649231212572

Yu, P., Tan, X., & Dimarogonas, D. V. (2024). Continuous-time control synthesis under nested signal temporal logic specifications. *IEEE Transactions on Robotics*, *40*, 2272–2286. https://doi.org/10.1109/TRO.2024.3353081

Zhang, W. T., Chi, M., Liu, Z. W., & Xu, J. Z. (2026). Distributed execution of signal temporal logic tasks in open networked robotic system via predefined-time control. *IEEE Transactions on Automation Science and Engineering*, *23*, 2969–2982. https://doi.org/10.1109/TASE.2026.3658586

Zhang, Y., Jiang, T., Cai, Z., & Ji, Y. (2026). Safety-critical control under timed reach-avoid specifications: A backup control barrier function approach. *IEEE Control Systems Letters*, *10*, 109–114. https://doi.org/10.1109/LCSYS.2026.3665795

Zhou, C., Yang, J., Li, S., & Chen, W. H. (2025). Temporal logic disturbance rejection control of nonlinear systems using control barrier functions. *IEEE Transactions on Cybernetics*, *55*(3), 1008–1017. https://doi.org/10.1109/TCYB.2024.3515456

Zhu, G., & Long, L. (2025). Safety-critical dynamic event-triggered control for signal temporal logic tasks with high-order control barrier functions. *International Journal of Systems Science*, *57*(13), 4328–4341. https://doi.org/10.1080/00207721.2025.2601779